

EXPERIMENTAL STUDY ON PILE STRESS IN LIQUEFIED AND LATERALLY SPREADING SOILS

Naohito ADACHI¹, Yasutugu SUZUKI² And Tsunehisa TSUGAWA³

SUMMARY

An experimental study on Soil-Pile-Structure interaction model is conducted by shaking table tests in order to evaluate the pile stress induced by liquefied soil and by laterally spread soil. Due to the quay wall placed near piles, lateral spread of soil gives subsequent effects on the pile foundation as well as liquefaction. Several experimental findings are: (1) Soil surrounding piles acts as a seismic resistance by collaborating with piles before liquefaction, while after liquefaction, it causes a pile shear force at the layer boundary six times larger than the external force at the pile head. (2) Interactive force between soil and pile is large and is attributed to the relative displacement between them before liquefaction, while it is small and is attributed to the relative velocity after liquefaction. (3) Under the laterally spreading soil condition, soil resistance acting together with a pile largely varies corresponding with the distance from the quay wall.

INTRODUCTION

In the Hyogoken-Nanbu (Kobe) Earthquake in Japan of January 17, 1995, pile foundation structures built on seaside and reclaimed lands were severely damaged by soil liquefaction and lateral spreading. Intensive damage surveys^{1, 2)} conducted after the earthquake found that these piles were damaged not only at their heads due to the inertial force of the superstructure but also at the intermediate depth of the liquefied soil due to unexpected external forces induced by large soil deformations. Damages were also found at the layer boundary between liquefied and non-liquefied soils.

The present study covers experimental conditions varying from non-liquefied, partially liquefied and/or completely liquefied soils to laterally spreading soils, using a saturated soil model. The soil model constructed in the laminar container has an unprecedented two-layer composition of an upper liquefiable soil and a lower non-liquefiable soil. The pile foundation model with superstructure is installed in this soil model. A quay wall adjacent to the pile foundation is also modeled and added in order to induce the lateral spreading. Pile stresses, reactive forces of soil, and other influential characteristics under various conditions subjected to shaking table excitations are found as experimental results and discussed from practical viewpoints for seismic design.

EXPERIMENTAL PROCEDURE

The laminar container used in the experiments consists of ten vertically stacked identical frames, 6 cm each in height. The width, depth, and height of the container inside are 1.2, 0.8, and 0.6 m, respectively. Two experimental models are built. Model 1 is Soil- Pile-Structure interaction model and Model 2 has an additional quay wall model installed adjacent to the pile foundation in Model 1. The whole model and measuring sensor locations for Model 2 are shown in Figure 1.

The upper soil of these models is made of saturated Iwami-gin sand³⁾, while the silicone rubber substitutes for the lower soil. Saturation is fulfilled by fully agitating and by boiling the sand into a loose condition and then by shaking it applying white noise excitation to create a homogeneous sand layer with a relative density of about

¹ Kajima Technical Research Institute, Tokyo, JAPAN E-mail:naohito@katri.kajima.co.jp

² Kajima Technical Research Institute, Tokyo, JAPAN E-mail:suzuki@katri.kajima.co.jp

³ Kajima Technical Research Institute, Tokyo, JAPAN E-mail:tsugawa@katri.kajima.co.jp

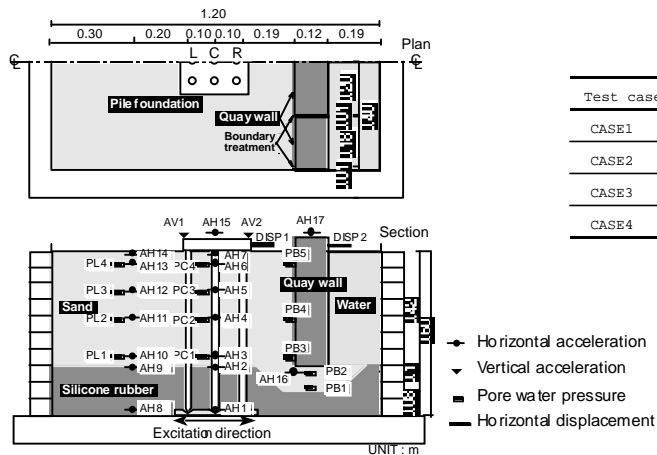


Figure 1 Test model and measuring sensor locations

TABLE 1 THE EXPERIMENTAL CASES

Test case	Test model	Input wave	Input acc. level (cm/s ²)	cm/s/Number of test	
CASE1	MODEL1	Lateral loading test i0	32.7N	1	
CASE2			50	500	7
CASE3	MODEL2	RINKAI92	50	500	29
CASE4			50	600	17

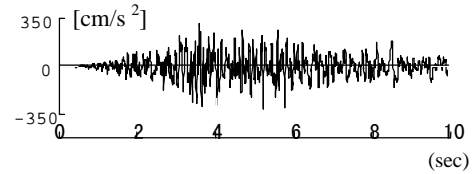


FIGURE 2 INPUT WAVE

60%. The shear stiffness of silicone rubber is processed to have an average initial shear stiffness ($G_0 = 4.9 \text{ MN/m}^2$) identical to that of the saturated sand if located at the same depth in the lower layer. These two layered soils are, therefore, considered as the initial soil condition before shaking. In the case of making Model 2, the initial soil is created with the quay wall fixed with jigs.

Referring to one bay of an actual five-story reinforced concrete building, nine acrylic tubes make the pile foundation model, with three rows and three lines supporting a superstructure weighing 137 N, equivalent to 2.2 MN of an actual building. The ratio of similarity⁴⁾ is decided to be 25. Each tube pile has 25 mm in diameter, 3 mm in thickness and 595 mm in length, equivalent to an actual steel pile of 0.6 m in diameter and 9 mm in steel thickness. The piles are rigidly connected to each other at the pile head while pin-supported at the tip in the bottom of the container.

Three steel boxes, one measuring 40 cm wide, 12 cm deep and 47 cm high, and the other two 18 cm wide, 12 cm deep and 48 cm high, model the quay wall. Their apparent specific gravity is about 2.1, almost the same as that of the actual concrete quay wall. The gaps in between the steel boxes and between steel boxes and container walls are filled with sponge-based tapes to reduce friction and to prevent sand spillage.

Horizontal and vertical accelerations, pore water pressures, and displacements are measured as well as pile strains. The pile strains are measured in the excitation direction in order to estimate bending stresses at the central piles. Strain measurements are made at 12 points in the pile C of Model 1, while at 8 points in each pile (pile R, C, and L) of Model 2⁴⁾.

The numbers of the experimental cases are shown in Table 1. In case 1, the pile head is horizontally loaded by a special actuator placed at the top level of the container. In case 2, the upper soil is fully replaced by water to observe structural behaviors of the pile foundation as simply but practically assumed in design practices. In case 3, the upper layer is to be partially or fully liquefied depending on the wide range of shaking intensities. In case 4, the upper layer is to be further laterally spread. The artificial earthquake wave (RINKAI92)⁵⁾, used in present design practice for the southern part of Kanto region in Japan, is applied as the input acceleration wave after condensing the time scale to one-fifth and varying the maximum intensity. Acceleration excitation is applied for 24 seconds by the shaking table, a 10-second duration pattern of which is shown in Figure 2. In order to obtain the successive and sequentially distributed data over varied intensities, the test numbers as listed in the Table 1.

EXPERIMENTAL RESULTS

Response characteristics of soil and superstructure

Figure 3 shows the distributions of excess pore water pressure in the soil in cases 3 and 4. In case 3, the soil is partially liquefied at an acceleration intensity of 150 cm/s^2 and is almost completely liquefied at 200 cm/s^2 . In case 4, the soil also begins to liquefy at 150 cm/s^2 but mostly liquefies at a greater intensity of 400 cm/s^2 .

As examples of response results of cases 3 and 4, Figure 4 shows the response time histories. Structure response acceleration (AH15), structure response displacement (DISP1), soil surface acceleration (AH14), and excess pore water pressure at the soil surface (PL4) during 10 seconds excitations from the beginning are illustrated for the acceleration intensities of 150 and 400 cm/s^2 . In Model 2, the maximum input acceleration of 150 cm/s^2

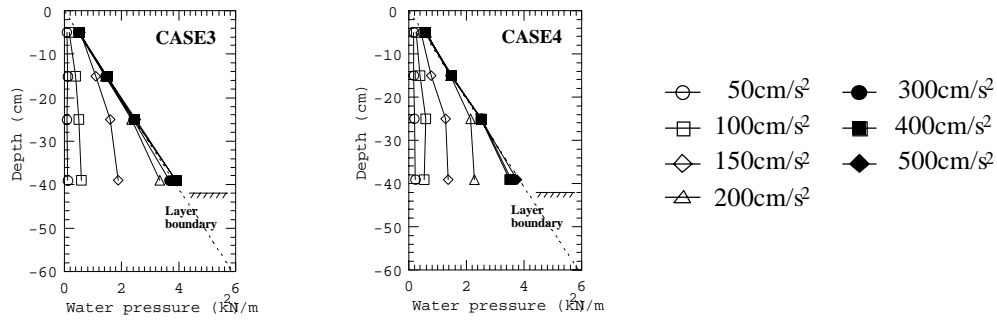


Figure 3 Distributions of maximum excess pore water pressure

corresponds to the partially liquefied condition while 400 cm/s^2 corresponds to the completely liquefied condition. It is recognized that the quay wall nearly tilts over during the excitations and that the residual displacements at the top of the quay wall after excitation are 4.5 and 89.0 mm, respectively.

At the maximum input acceleration of 150 cm/s^2 in case 3 under partially liquefied condition, it is remarkable that the ground soil acceleration wave shows pulse-like response and the structure response displacement increases during 4 to 7 seconds when the soil starts to liquefy. In case 4, the pore water pressure does not rise so much as in case 3 but clearly recovers due to the possible effect of cyclic mobility while the structure is somewhat residually deformed toward the quay wall. At the maximum input acceleration of 400 cm/s^2 whereby the ground soil is completely liquefied, liquefaction starts at about 4 seconds in case 3, and there appears to be no significant acceleration duration at the surface, while the response acceleration and displacement of the structure increase about 6 seconds after the beginning. In case 4, the soil liquefies at 4 seconds, but the pore water pressure then slightly decreases with the movement of the quay wall. Like in case 3, the ground surface responds little to the input acceleration from 4 seconds, and the structure at first deforms largely toward the quay wall then returns back. After the return of the structure, large pulses are produced on the structure response acceleration. This can be regarded as another effect of cyclic mobility.

The maximum response acceleration of the ground surface and the structure is slightly smaller in case 4 than in

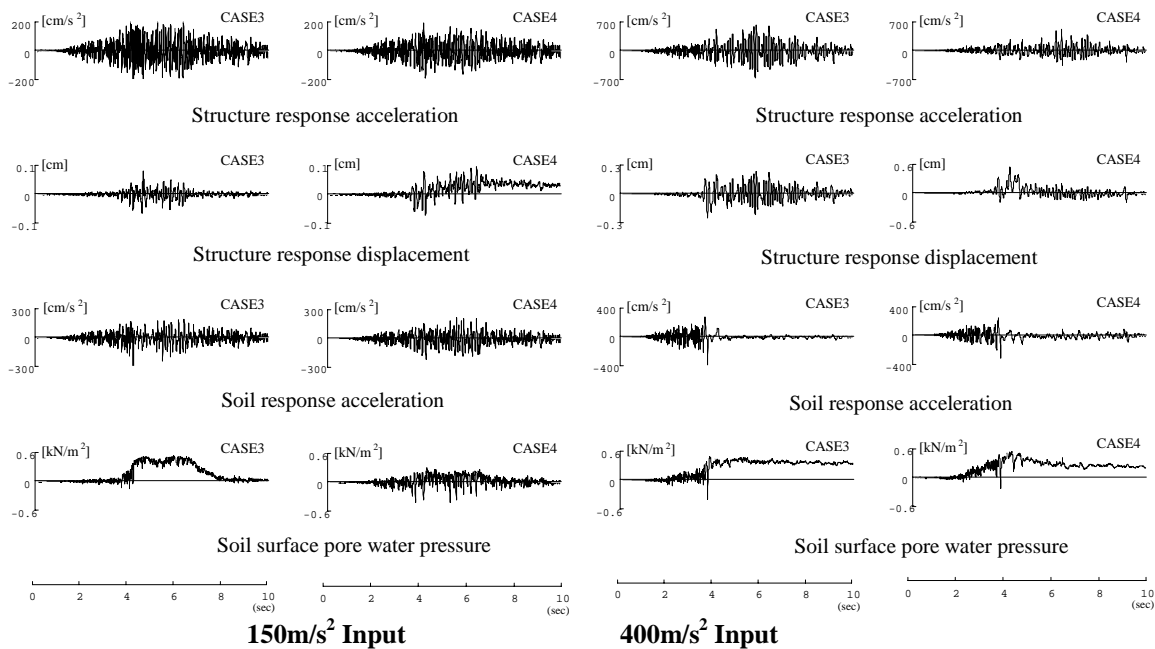


Figure 4 Response time histories at soil and superstructure

case 3, but the response displacement of the structure is greater in case 4 than in case 3. In case 4, the structure largely moves toward the quay wall with the movement of the quay wall. This movement of the structure remains as residual deformation in the partially liquefied condition, but the residual deformation is virtually zero

in the completely liquefied condition. This is probably because the resistance of the ground to restoration is small in the completely liquefied condition.

Response characteristics of piles

The maximum bending moment distributions of the center pile C from cases 1 to 4 are shown in Figure 5. The maximum bending moment at each depth occurs either at 4 seconds after excitation, when the ground displacement becomes the maximum, or at 6 seconds, when the structure inertial force becomes the maximum. In Figure 5, all the bending moments are represented provided that the bending moment of the pile head is defined and expressed as positive in which the structure is displaced with maximum value in an either direction. That is, the maximum values of bending moment at each depth that may occur at different times are represented in the form of the deformation mode.

The bending moment of the pile increases not only at the pile head but also at the boundary between the saturated sand and the silicone rubber (hereinafter referred to as the layer boundary) in all cases except case 1. In case 2, in which the upper layer is water, the force imposed by the upper water layer is so small that the bending moment of the pile changes linearly from the head to the layer boundary. Due to the fact that the pile head is completely fixed while the layer boundary is semi-fixed by the elastic silicone rubber, the bending moment of the pile at the layer boundary is about 80% of that of the pile at the head. When the upper layer is non-liquefied in cases 3 and 4, the bending moment of the pile occurred at the layer boundary is smaller than that of the pile at

(Fig.5~Fig.7) CASE1 □ 5.4N ● 21.8N CASE2~4 □ 100cm/s² △ 200cm/s² ■ 400cm/s²
 ○ 2.7N △ 10.9N ■ 32.7N ○ 50cm/s² ◇ 150cm/s² ● 300cm/s² ◆ 500cm/s²

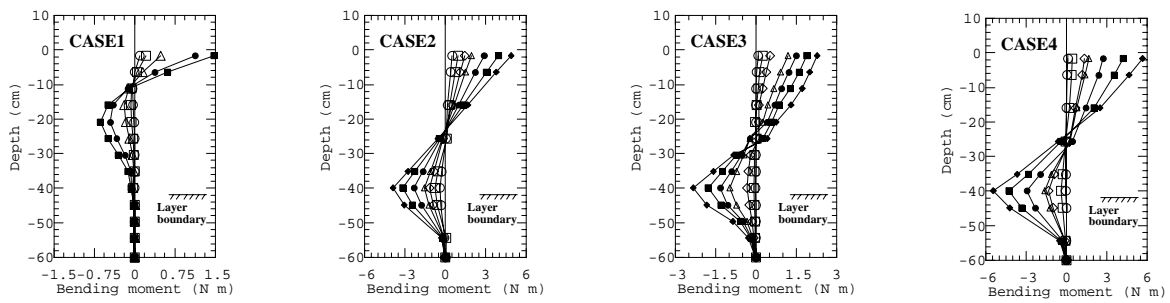


Figure 5 Distributions of maximum bending moment for Pile-C

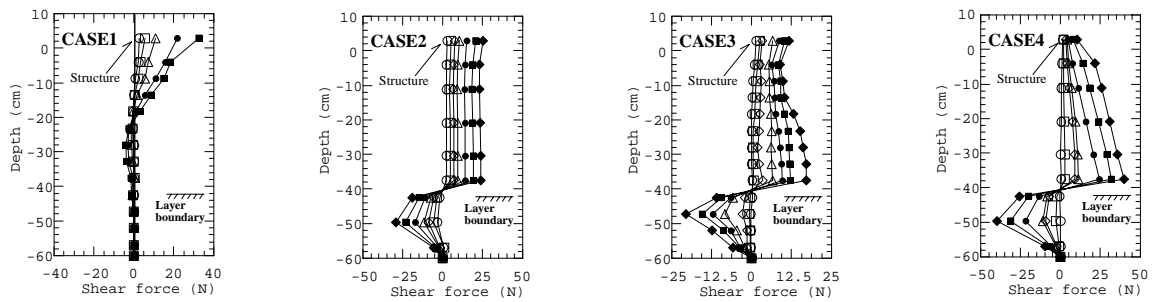


Figure 6 Distributions of maximum shear force for Pile-C

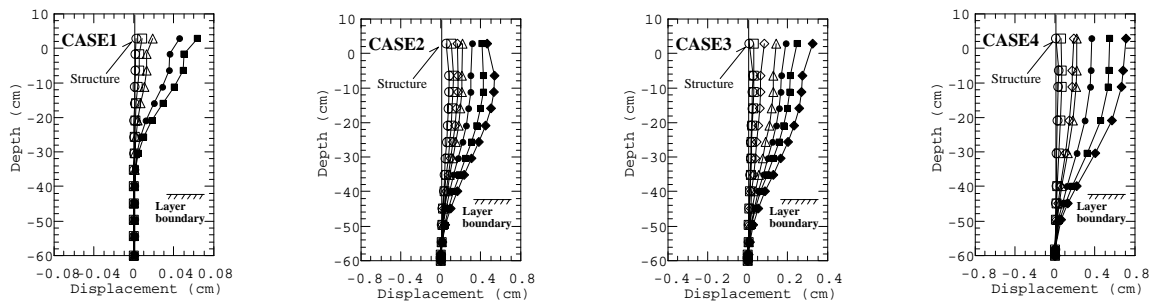


Figure 7 Distributions of maximum lateral displacement for Pile-C

the head like in case 1. On the other hand, when the ground is partially or completely liquefied in both cases 3 and 4, the bending moment of the pile at the layer boundary becomes almost the same as that of the pile at the head. When the upper layer liquefies or laterally spreads the bending moment of the pile at the layer boundary is slightly larger than that in the case in which the upper layer is water. The bending moments of the pile at the head and at the layer boundary in case 4 are two times larger than in case 3 under the influence of the lateral spreading of the upper soil layer due to the movement of the quay wall.

The maximum shear force distributions of the center pile C, computed and obtained by differentiating the bending moment time histories, are shown in Figure 6. In this figure, the inertial force of the superstructure represents shear force at the pile head. The maximum lateral displacement distributions of the center pile C, also obtained by double integrating strain time histories under the assumption that the horizontal displacement of the pile tip is zero, are shown in Figure 7. The lateral displacement (DISP1) measured on the structure is also shown in Figure 7.

In case 2, in which the upper layer is water, the inertial force of the structure is directly transferred to the lower layer, and a shear force in the negative direction is produced in the lower layer. This indicates that the force induced by water is very small regardless of the input acceleration level. In both case 3 and 4, when the upper layer is non-liquefied (the input acceleration is 50 cm/s^2), the upper shear force beneath the pile head is also small like in case 1. This indicates that the ground soil acts as a reaction to the pile throughout the whole length. However, if the ground is partially or completely liquefied under the input acceleration from 150 to 500 cm/s^2 , the shear force from the pile head to the layer boundary increases in case 3 and especially in case 4. By comparing the forces in case 3 with those in case 4, it is clearly recognized that the laterally spread soils induced by the movement of quay wall possibly produce far higher stresses in the piles at the head and layer boundary, up to twice than by the sole liquefaction. Regarding the pile displacement, it is recognized by comparison of case 2 with case 3 that the liquefied soil increases the pile deformation under the influence of soil deformation as well as the water, but is more effective in limiting the amount of pile deformation than the water.

Damage investigation and related analytical studies on structures after the 1995 Hyogoken-Nanbu Earthquake have revealed that when the ground is laterally spread by the movement of quay walls, the movement of the ground varies with the distance from the quay walls, and that the pile reaction also differs each other. The maximum bending moment and shear force distributions occurred at three piles, R, C, and L at different distances from the quay wall in case 4 with an input acceleration of 400 cm/s^2 are compared in Figure 8. The maximum bending moment distribution of the pile R nearest to the quay wall is clearly different in shape from those of piles C and L, because pile R is greatly pushed by the ground. This tendency is made clearer in the distribution of the shear force. Due to the movement of quay wall, a shear force in the direction opposed to that of the inertial force of the structure is produced in the head of pile R, and the shear force of pile R at the layer boundary is greater than those of the other two piles. It has been pointed out by Tokimatsu et al (1997)⁶⁾ that, although piles in a group are fixed at the head, individual pile is subjected to different force each other from the surrounding ground. Therefore it should be noticed that an excessive shear force acting at the head of the pile nearest to the quay wall possibly occurs if the direction of the external force imposed by the ground on the piles is opposite to the direction of the inertial force of the piles.

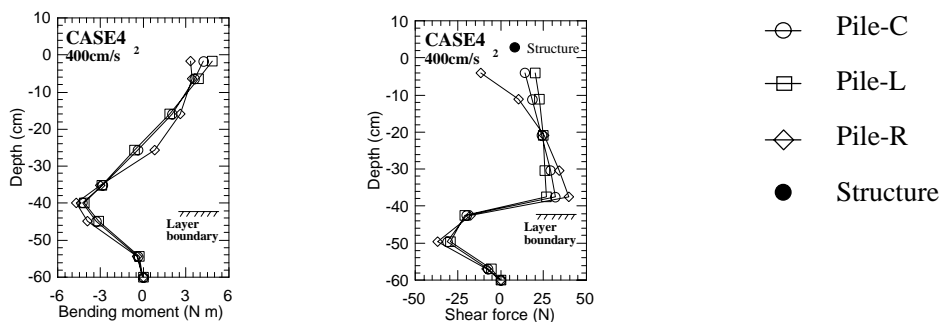


Figure 8 Distributions of maximum bending moment and shear force for C, L and R-pile

Relationships between pile stresses and input accelerations

The relationships between the maximum bending moment and shear force of the piles at the head and at the layer boundary and the maximum input accelerations are shown for cases 3 and 4 in Figure 9. For the convenience of comparison, both bending moment and shear force are generalized and expressed in the form of a ratio by

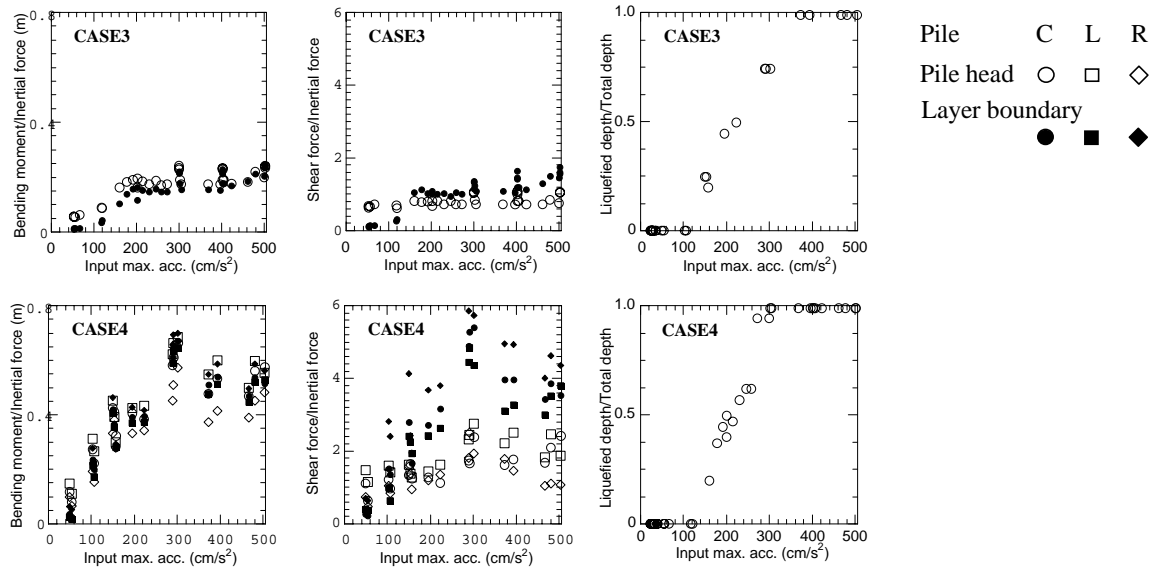


Figure 9 Relationships between pile stresses and input accelerations

dividing both of them by the maximum inertial force occurred in the super structure. The data shown are for the center pile C alone in case 3 and for three piles L, C and R in case 4. The relationships between the ratio of liquefied depth to the whole sand layer depth and the maximum input accelerations are also shown in the figure, which shows that no liquefaction happens at less than 100 cm/s^2 in both cases 3 and 4 while the whole sand layer liquefies at more than 300 and 400 cm/s^2 in cases 3 and 4, respectively.

In case 3, the bending moment ratio is almost proportional to the maximum input acceleration up to 150 cm/s^2 keeping the transient condition from the non-liquefied stage to the partially liquefied stage, while it becomes almost constant if the maximum input acceleration exceeds about 150 cm/s^2 . It is noticeable that, under the maximum input acceleration of less than 300 cm/s^2 , after the completely liquefied condition occurs, the bending moment of the pile at the head is larger than that of the pile at the layer boundary. But, when the maximum input acceleration exceeds 300 cm/s^2 , it becomes difficult to recognize any significant difference between the bending moment ratio at the head and at the layer boundary. The shear force ratio of the pile head is small under the small input acceleration but becomes almost unity after the maximum input acceleration exceeds about 150 cm/s^2 , indicating that the inertial force of the structure is directly replaced by the shear force at the pile head. The shear force of the pile at the head is greater than at the layer boundary under the maximum input acceleration below 150 cm/s^2 but becomes smaller under the maximum input acceleration exceeding 150 cm/s^2 .

In case 4, the ratios of both the bending moment and the shear force at the layer boundary increase as the maximum input acceleration increases up to about 300 cm/s^2 . This is attributed to the fact that the quay wall laterally moves, enforcing the ground sand to spread laterally. In fact, the shear force ratio of the pile at the head, which is estimated at the location of 4 cm below the head, is clearly greater than unity, due to the force imposed and added by the ground. When the ground is laterally spread as a result of the movement of the quay wall, the amount of the lateral spreading varies with the distance from the quay wall. The three piles at different distances from the quay wall thus have different distributions in bending moment and shear force. The pile-head bending moment of the pile R nearest to the quay wall is slightly smaller than that of the other two piles, and the three piles are remarkably different from each other in shear force. The pile L farthest from the quay wall has the largest pile-head shear force, whereas the pile R nearest to the quay wall has the largest layer-boundary shear force. It should be remarked that, under the input acceleration of 400 cm/s^2 or more when the ground sand is completely liquefied, these ratios are not so large as before. This is possibly because the large pulse-like acceleration of the structure induced by the influence of cyclic mobility of sand happens to issue large inertial force even under the completely liquefied state.

By comparison of pile stresses at the head with those at the layer boundary, it should be noticed that the bending moment and shear force of the pile at the layer boundary are smaller than those of the pile at the pile head where the ground is non-liquefied. However, if the upper layer is liquefied, the bending moment of the pile at the layer boundary becomes almost same as that of the pile at the head, and the shear force of the pile at the layer boundary becomes about 1.5 times larger than that of the pile at the pile head. Furthermore, if the ground sand laterally spreads, the maximum stresses of the pile R nearest to the quay wall at the layer boundary become

about three times larger in bending moment and six times larger in shear force than those at the pile head.

CHARACTERISTICS OF REACTION FORCES BY SOIL

Maximum reaction force distributions

The maximum reaction force distributions obtained by further differentiating the shear force time histories of the piles are shown in Figure 10 for the center pile C in case 3 and for the three piles L, C and R in case 4. The reaction force of each pile increases almost in proportion to the input acceleration. The reaction forces of pile C in case 3 at the lower part are larger when partially liquefied under the input acceleration from 150 to 200 cm/s^2 while smaller when completely liquefied under the input acceleration from 300 to 500 cm/s^2 than forces at the upper part of the sand. The piles L, C and R in case 4 exhibit, in general, similar tendencies to those observed in case 3 through all the stages from partially liquefied to completely liquefied conditions under the input acceleration from 150 cm/s^2 to 500 cm/s^2 . However, it is to be pointed out that the reaction force of center pile C has little change even though the input acceleration rises after complete liquefaction, while the reaction forces of Pile L are smaller under the acceleration of 500 cm/s^2 than those under the acceleration of 400 cm/s^2 , and that the Pile R located nearest to the quay wall is subjected to much larger reaction forces than those of the other piles.

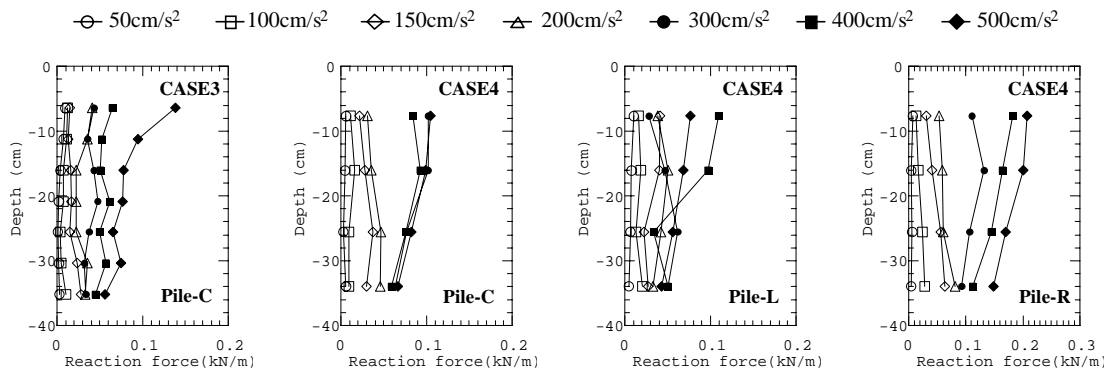


Figure 10 Distributions of maximum reaction force of piles at saturated sand layer

Relationships between reaction force and relative displacement/velocity

When evaluating the external forces imposed on piles by liquefied and laterally spread soils, some researchers assume that the ground soil is solid and that the seismic force occurs in relation to the relative displacement between the piles and soil ⁶⁾, while other researchers presume that soil is fluid and that the external force occurs in proportion to the relative velocity between the piles and soil ⁷⁾. To clarify whether the force imposed by the soil on the piles arises by displacement or by velocity, the experimental results of case 3 under the maximum input acceleration of 400 cm/s^2 at the depth of 6.4 cm are represented in the form of the time histories of, the reaction force to the piles, relative displacement and velocity between soil and piles as well as of excess pore water pressure in soil as shown in Figure 11. It is recognized that the relative displacement and relative velocity sharply increase as the excess pore water pressure generates.

The relationships between the reaction force and relative displacement/velocity are shown in Figure 12 after dividing the whole time duration into the three time ranges of 0 to 3 seconds when the excess pore water pressure is still low, 3 to 4.5 seconds when the excess pore water pressure is rising, and 4.5 to 11 seconds when the ground continues to liquefy. In the time range of 0 to 3 seconds, the reaction force and relative displacement are correlated slightly positively. In the time range of 3 to 4.5 seconds, the reaction force and relative displacement trace triangular loops. This is considered to be a cyclic mobility phenomenon in which the reaction force is close to zero when the relative displacement is small and increases when the relative displacement exceeds a certain level. In the time range of 4.5 to 10 seconds, a tendency similar to that observed in the time range of 3 to 4.5 seconds is noted, but not a good correlation is recognized between the reaction force and relative displacement. On the other hand, the reaction force and relative velocity are not correlated in the time range of 0 to 3 seconds, but are correlated positively in the latter half of the time range of 3 to 4.5 seconds, and force correlates well with the relative displacement before liquefaction and correlates well with the relative velocity after liquefaction.

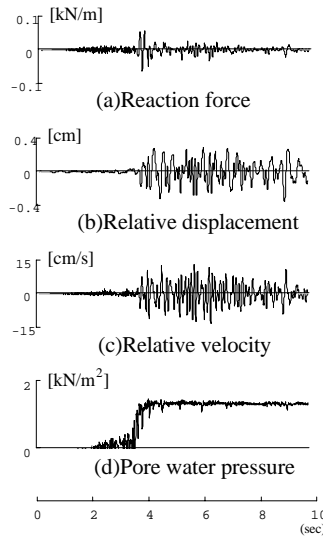


Figure 11 Response time histories of pile at 6.4cm deep (CASE3)

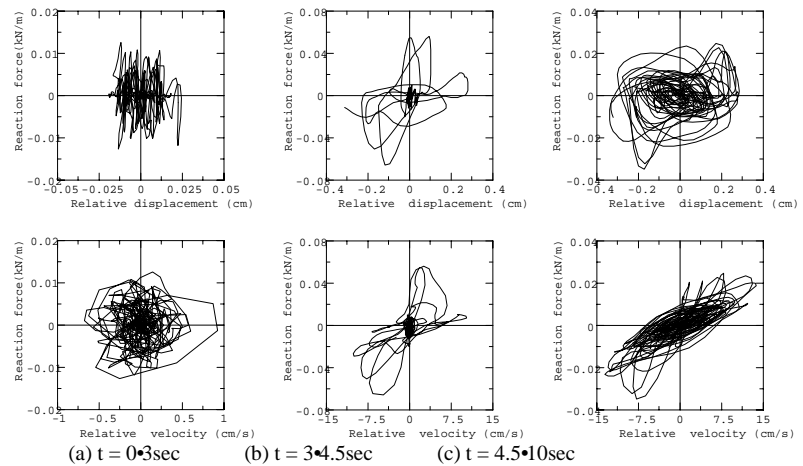


Figure 12 Relationships between reaction force and relative displacement/velocity (CASE3)

CONCLUSIONS

The concluding remarks of this study are as follows:

1. Soil surrounding piles acts as a seismic resistance by collaborating with piles before liquefaction, while after liquefaction, it causes a pile shear force at the layer boundary six times larger than the external force at the pile head.
2. Interactive force between soil and pile is large and is attributed to the relative displacement between them before liquefaction, while it is small and is attributed to the relative velocity after liquefaction.
3. Under the laterally spread soil condition, soil resistance acting together with a pile largely varies corresponding with the distance from the quay wall.

REFERENCES

1. Damage investigation commission on the Hanshin-Awaji earthquake, (1998), "Damage investigation on the Hanshin-Awaji earthquake, Structure Vol.4, Wooden building, Building foundation structure", Architectural Institute of JAPAN, pp.547. (in Japanese)
2. Committee on Building Foundation Technology against Liquefaction and Lateral Spreading, (1997), "Study on liquefaction and lateral spreading in the Hyogoken-Nanbu Earthquake", pp.593. (in Japanese)
3. Susumu Iai, (1989), "Similitude for shaking table tests on soil-structure-fluid model in 1g gravitational field", Soils and Foundations, Vol.29, No.1, pp.105-118.
4. Suzuki Yasutsugu, Naohito Adachi, (1999), "Relationship between reaction force and relative displacement in liquefied and laterally spreading soils" A symposium on liquefaction mechanism and prediction/design method, The Japanese Geotechnical Society, pp.531-538. (in Japanese)
5. Masanori Niwa, et al. (1991), "Study on Strong Motion Design Basis in Tokyo Coastal Area", Summaries of Technical Papers of Annual Meeting Architectural Institute of JAPAN, Structure-I, pp.361-362. (in Japanese)
6. Kouji Tokimatsu, Hiroshi Ooka, Yasuhiro Shyamoto, (1997), "Destruction and deformation mode of piles induced by laterally spreading in the Hyogoken-Nanbu Earthquake" Journal of Structural and Construction Engineering, Vol.495, pp.95-100. (in Japanese)
7. Masanori Hamada, Kazue Wakamatsu, (1998), "Study on lateral displacement of the soils induced by liquefaction", Journal of Geotechnical Engineering, No.596, pp.189-208. (in Japanese)